A (π-Extended Tetrathiafulvalene)−Fluorene Conjugate. Unusual Electrochemistry and Charge Transfer Properties: The First Observation of a Covalent D 2+ −σ−A • − Redox State 1

ARTICLE *in* JOURNAL OF THE AMERICAN CHEMICAL SOCIETY · DECEMBER 2002

Impact Factor: 12.11 · DOI: 10.1021/ja012518o · Source: PubMed

J|A|C|S
ARTICLES
Published on Web 10/30/2002

A (π-Extended Tetrathiafulvalene)−Fluorene Conjugate. Unusual Electrochemistry and Charge Transfer Properties: The First Observation of a Covalent $D^{2+}-\sigma-A^{\bullet-}$ Redox State[1]

Dmitrii F. Perepichka,[†] Martin R. Bryce,*[,†] Igor F. Perepichka,[‡] Svetlana B. Lyubchik,[‡] Christian A. Christensen,[†] Nicolas Godbert,[†] Andrei S. Batsanov,[†] Eric Levillain,[§] Eric J. L. McInnes,[||] and Jing P. Zhao[||]

Contribution from the Department of Chemistry, University of Durham, Durham DH1 3LE, U.K., L. M. Litvinenko Institute of Physical Organic and Coal Chemistry, National Academy of Sciences of Ukraine, Donetsk 83114, Ukraine, Ingénierie Moléculaire et Matériaux Organiques, CNRS UMR 6501, Université d'Angers, 49045 Angers Cedex 01, France, and the EPSRC c.w. EPR Service Centre, Department of Chemistry, The University of Manchester, Manchester MI3 9PL, U.K.

Received November 9, 2001

Abstract: The synthesis of novel electrochemically amphoteric TTFAQ−σ−A compounds (TTFAQ = 9,10-bis(1,3-dithiol-2-ylidene)-9,10-dihydroanthracene, σ = saturated spacer, A = polynitrofluorene acceptor) is reported. Their solution redox behavior is characterized by three single-electron reduction and one two-electron oxidation waves. Electrochemical quasireversibility of the $TTFAQ^{2+}$ state and a low $E_{ox} - E_{red}$ gap ($\approx$0.25 V) for 3-(9-dicyanomethylene-4,5,7-trinitrofluorene-2-sulfonyl)-propionic acid 2-[10-(4,5-dimethyl-[1,3]dithiol-2-ylidene)-9,10-dihydroanthracen-9-ylidene]-5-methyl-[1,3]dithiol-4-ylmethyl ester (**10**) has enabled the electrochemical generation of the hitherto unknown transient $D^{2+}-\sigma-A^{\bullet-}$ state as observed in cyclic voltammetry and time-resolved spectroelectrochemistry. The ground state of compound **10** was shown to be ionic in the solid but is essentially neutral in solution (according to electron paramagnetic resonance). The X-ray structure of an intermolecular 1:2 complex between 2-[2,7-bis(2-hydroxyethoxy)-9,10-bis(4,5-dimethyl-[1,3]dithiol-2-ylidene)-9,10-dihydroanthracene and 2,5,7-trinitro-4-bromo-9-dicyanomethylene-fluorene, **14**·(**17**)$_2$, reveals, for the first time, full electron transfer in a fluorene charge-transfer complex.

Introduction

Multistage organic redox systems and, in particular, electrochemically amphoteric compounds, for which both oxidized and reduced states are available within a readily accessible potential window, are of current interest in both theoretical and experimental research due to their potential applications in molecular electronics and optoelectronics.[2−4]

There are two basic strategies to endow high electrochemical amphotericity: (i) by extending π-conjugation in the molecule (in the ultimate case of graphite $E_{ox} - E_{red} = 0$ V) and (ii) by construction of covalent donor−acceptor (D−A) compounds in which the highest occupied molecular orbital (HOMO) and lowest unoccupied molecular orbital (LUMO) orbitals are essentially separated and, therefore, can be independently tuned to achieve the required values of E_{ox} and E_{red}. The first strategy is realized in the design of linear π-conjugated polymers and oligomers, where the main synthetic principles of band gap control have now been substantially formulated. They include an increase in the quinoid character of the conjugated system due to a decrease in its aromaticity, the rigidification of the conjugated system into a nearly planar conformation, and the creation of alternating electron-donating and electron-accepting fragments along the conjugated chain.[5] The second strategy, which is realized for molecular D−σ−A systems, generally explores a systematic choice of D and A units and the introduction of electron-donating and electron-withdrawing substituents at appropriate sites to tune independently the HOMO and LUMO levels. Although it was widely used in the design of intramolecular charge-transfer materials,[6] high amphotericity ($E_{ox} - E_{red} < 0.5$ V) is quite unusual for closed-shell organic molecules.[3b,7] To achieve this, strong electron-donor and strong electron-acceptor fragments should be linked,

* Address correspondence to this author. E-mail: m.r.bryce@durham.ac.uk
† University of Durham.
‡ National Academy of Sciences of Ukraine.
§ Université d' Angers.
|| University of Manchester.

(1) (a) Electron Acceptors of the Fluorene Series, Part 14. Part 13 see: Perepichka, I. F.; Perepichka, D. F.; Lyubchik, S. B.; Bryce, M. R.; Batsanov, A. S.; Howard, J. A. K. *J. Chem. Soc., Perkin Trans. 2* **2001**, 1546−1551. (b) Molecular Saddles, Part 9. Part 8 see: Godbert, N.; Bryce, M. R. *J. Mater. Chem.* **2002**, *12*, 27−36.
(2) Nakasuji, K.; Yoshida, K.; Murata, I. *J. Am. Chem. Soc.* **1983**, *105*, 5136−5137.
(3) (a) Tsubata, Y.; Suzuki, T.; Miyashi, T. *J. Org. Chem.* **1992**, *57*, 6749−6755. (b) Suzuki, T.; Miyanari, S.; Tsubata, Y.; Fukushima, T.; Miyashi, T.; Yamashita, Y.; Imaeda, K.; Ishida, T.; Nogami, T. *J. Org. Chem.* **2001**, *66*, 216−224.
(4) (a) Hünig, S.; Kemmer, M.; Wenner, H.; Perepichka, I. F.; Bäuerle, P.; Emge, A.; Gescheid, G. *Chem. Eur. J.* **1999**, *5*, 1969−1973. (b) Hünig, S.; Kemmer, M.; Wenner, H.; Barbosa, F.; Gesheidt, G.; Perepichka, I. F.; Bäuerle, P.; Emge, A.; Peters, K. *Chem. Eur. J.* **2000**, *6*, 2618−2632.
(5) Roncali, J. *Chem. Rev.* **1997**, *97*, 173−205.
(6) Bryce, M. R. *Adv. Mater.* **1999**, *11*, 11−23.

Chart 1

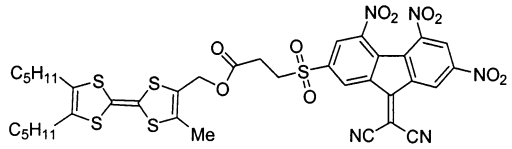

but this approach faces a number of experimental hindrances.[8] The conjunction of a strong donor (e.g., tetrathiafulvalene (TTF)) and a strong acceptor (e.g., 7,7′,8,8′-tetracyano-*p*-quinodimethane (TCNQ)) in a D−σ−A system has been a challenge[9] since an inspiring proposal for unimolecular rectification in a TTF−σ−TCNQ molecule.[10]

This class of molecules has attracted our recent interest[8b,11] due to their potential to act as unimolecular rectifiers,[10] single-component electrical conductors,[3a,7,12] molecular switches,[13] and artificial photosynthetic centers based upon intramolecular photoinduced electron transfer.[14] We recently reported a TTF−σ−A diad **1** (Chart 1) where A is a polynitrofluorene moiety with a high electron affinity (similar to TCNQ).[11b] Compound **1** possessed six reversible redox states, and the value $E_{ox}^0 - E_{red}^0$ was as low as 0.3 V. In this context our attention was drawn to an "extended" TTF donor with anthraquinoidal separation of the two 1,3-dithiole units (TTFAQ) due to its ability to release two electrons, simultaneously, in one quasi-reversible process. This quasireversibility[15] is due to the marked structural rearrangement which accompanies the redox process between a strongly bent (saddle shaped) neutral state and a fully aromatic dication species in which the anthracene nucleus is planar with the dithiolium rings orthogonal.[16] Such a peculiarity of TTFAQ donors could lead to unusual electrochemical behavior in highly amphoteric D−σ−A systems. There are a few reports on the attachment of the TTFAQ system to different acceptor moieties, viz., fullerene,[17] porphyrin (as well as TTFAQ-porhyrin-C_{60} triad),[14b] 11,11,12,12-tetracyanoanthraquinodimethane,[18] 1,4-naphthoquinone,[19] and a dicyanovinyl group[20] (which possess moderate electron affinity).

Here we report the synthesis and properties of the first TTFAQ−σ−fluorene diads **9** and **10** and fluorene−σ−TTFAQ−σ−fluorene triads **19** and **20**. The strong electron affinity of the fluorene fragment in compound **10** enriches the redox properties, providing high amphotericity ($E_{ox} - E_{red} \approx 0.25$ V), and a hitherto unknown redox state $D^{2+}-\sigma-A^{\bullet-}$ has been observed in cyclic voltammetry (CV) and time-resolved spectroelectrochemistry (SEC) experiments. The X-ray crystal structure of the TTFAQ/fluorene intermolecular complex **14**·(**17**)$_2$ reveals, for the first time, complete electron transfer in a charge-transfer complex (CTC) of a fluorene acceptor.

Results and Discussion

Synthesis. The synthesis of diads **9** and **10** is presented in Scheme 1. The 2-nitro group in fluorenone **2** was selectively substituted with 3-mercaptopropionic ester in acetonitrile solution in the presence of $NaHCO_3$ (as a basic catalyst and as a trap for the nitronic acid formed during the reaction). These conditions were found to be superior to those described by us recently for the reaction with *n*-butanethiol where aprotic dipolar solvents and no catalyst were used.[21] The sulfide **3** was oxidized to sulfone **4** with hydrogen peroxide in acetic acid, and the ester group was then converted to the acid **5** by treatment with aqueous trifluoroacetic acid and then to acid chloride **6** by treatment with oxalyl chloride. The overall yield of **6** in the above four steps was 70%. This acid chloride was coupled with hydroxymethyl-TTFAQ derivative **8**[22] with pyridine catalysis yielding TTFAQ-fluorenone conjugate **9** in 65% yield. To increase its acceptor ability, **9** was converted into the dicyanomethylene derivative **10** by reaction with malononitrile in DMF solution. For comparison, dicyanomethylene derivative **7** was synthesized from **4**. To obtain a single crystal of an intermolecular complex of TTFAQ with fluorene, variously substituted donor and acceptor components were explored and a successful combination was TTFAQ derivative **14** (Scheme 2) and a bromo-substituted fluorene acceptor **17** (Scheme 3). Compound **14** was coupled with **18** affording, in 60% yield, an A−σ−D−σ−A triad **19** and hence the dicyanomethylene derivative **20** (Scheme 4). However, a stronger acceptor, 2,5,7-trinitro-9-fluorenone-4-carbonyl chloride, gave only an oxidation product, i.e., salt $\mathbf{14}^{2+}\cdot 2Cl^-$ (90% yield) under these conditions.[23]

Electrochemistry. Compounds **9, 10, 19,** and **20** in CV experiments in MeCN and CH_2Cl_2 solutions show clear am-

(7) Suzuki, T.; Yamada, M.; Ohkita. M.; Tsuji, T. *Heterocycles* **2001**, *54*, 387−394.
(8) (a) Panetta, C. A.; Heimer, N. E.; Hussey, C. L.; Metzger, R. M. *Synlett* **1991**, 301−309. (b) de Miguel, P.; Bryce, M. R.; Goldenberg, L. M.; Beeby, A.; Khodorkovsky, V.; Shapiro, L.; Niemz, A.; Cuello, A. O.; Rotello, V. *J. Mater. Chem.* **1998**, *8*, 71−76.
(9) To date there is only one report on the coupling of substituted TTF and TCNQ: Panetta, C. A.; Baghdadchi J.; Metzger, R. M. *Mol. Cryst. Liq. Cryst.* **1984**, *107*, 103−113. However, a difficult synthetic route and problems with purification precluded detailed characterization of the compound.
(10) Aviram, A.; Ratner, M. *Chem. Phys. Lett.* **1974**, *29*, 277−283. For recent discussions of this proposal see: Metzger, R. M. *J. Mater. Chem.* **1999**, *9*, 2027−2036.
(11) (a) Perepichka, D. F.; Bryce, M. R.; Batsanov, A. S.; Howard, J. A. K.; Cuello, A. O.; Gray, M.; Rotello, V. M. *J. Org. Chem.* **2001**, *66*, 4517−4524. (b) Perepichka, D. F.; Bryce, M. R.; McInnes, E. J. L.; Zhao, J. P. *Org. Lett.* **2001**, *3*, 1431−1434.
(12) (a) Bando, P.; Martín, N.; Segura, J. L.; Seoane, C. *J. Org. Chem.* **1994**, *59*, 4618−4629. (b) Khodorkovsky, V.; Becker, J. Y. In *Organic Conductors. Fundamentals and Applications*; Farges, J.-P., Ed.; Marcel Dekker: New York−London−Hong Kong, 1994; pp 75−113. (c) Yamashita, Y.; Tomura, M. *J. Mater. Chem.* **1998**, *8*, 1933−1944.
(13) (a) Ashton, P. A.; Balzani, V.; Becher, J.; Credi, A.; Fyfe, M. C. T.; Mattersteig, G.; Menzer, S.; Nielsen, M. B.; Raymo, F. M.; Stoddart, J. F.; Venturi, M.; Williams, D. J. *J. Am. Chem. Soc.* **1999**, *121*, 3951−3957. (b) Nielsen, M. B.; Nielsen, S. B.; Becher, J. *Chem. Commun.* **1998**, 475−476. (c) Nielsen, M. B.; Hansen, J. G.; Becher, J. *Eur. J. Org. Chem.* **1999**, 2807−2815.
(14) (a) Gust, D.; Moore, T. A.; Moore, A. L. *Acc. Chem. Res.* **2001**, *34*, 40−48. (b) Kodis, G.; Liddell P. A.; de la Garza, L.; Moore, A. L.; Moore, T. A.; Gust, D. *J. Mater. Chem.* **2002**, *12*, 2100−2108.
(15) (a) Bryce, M. R.; Coffin, M. A.; Hursthouse, M. B.; Karaulov, A. I.; Müllen, K.; Scheich, H. *Tetrahedron Lett.* **1991**, *32*, 6029−6033. (b) Peréz, I.; Liu, S.-G.; Martín, N.; Echegoyen, L. *J. Org. Chem.* **2000**, *65*, 3796−3803. (c) Liu, S.-G.; Peréz, I.; Martín, N.; Echegoyen, L. *J. Org. Chem.* **2000**, *65*, 9092−9102.
(16) (a) Bryce, M. R.; Moore, A. J.; Hasan, M.; Ashwell, G. J.; Fraser, A. T.; Clegg, W.; Hursthouse, M. B.; Karaulov, A. I. *Angew. Chem., Int. Ed. Engl.* **1990**, *29*, 1450−1452. (b) Triki, S.; Ouahab, L.; Lorcy, D.; Robert, A. *Acta Crystallogr.* **1993**, *C49*, 1189−1192. (c) Bryce, M. R.; Finn, T.; Batsanov, A. S.; Kataky, R.; Howard, J. A. K.; Lyubchik, S. B. *Eur. J. Org. Chem.* **2000**, 1199−1205. (d) Jones, A. E.; Christensen, C. A.; Perepichka, D. F.; Batsanov, A. S.; Beeby, A.; Low, P. J.; Bryce, M. R.; Parker, A. W. *Chem. Eur. J.* **2001**, *7*, 973−978. (e) Christensen, C. A.; Batsanov, A. S.; Bryce, M. R.; Howard, J. A. K. *J. Org. Chem.* **2001**, *66*, 3313−3320.
(17) (a) Herranz, M. A.; Martín, N. *Org. Lett.* **1999**, *1*, 2005−2007. (b) Martín, N.; Sánchez, L.; Guldi, D. M. *Chem. Commun.* **2000**, 113−114.
(18) Herranz, M. A.; Gonzalez, S.; Perez, I.; Martín, N. *Tetrahedron* **2001**, *57*, 725−731.
(19) Christensen, C. A.; Bryce, M. R.; Batsanov, A. S.; Howard, J. A. K.; Jeppesen, J. O.; Becher, J. *Chem. Commun.* **1999**, 2433−2434.
(20) Herranz, M. A.; Martín, N.; Sánchez, L.; Garín, J.; Orduna, J.; Alcalá, R.; Villacampa, B.; Sánchez, C. *Tetrahedron* **1998**, *54*, 11651−11658.
(21) Perepichka, I. F.; Popov, A. F.; Orekhova, T. V.; Bryce, M. R.; Andrievskii, A. M.; Batsanov, A. S.; Howard, J. A. K.; Sokolov, N. I. *J. Org. Chem.* **2000**, *65*, 3053−3063.
(22) Godbert, N.; Bryce, M. R.; Dahaoui, S.; Batsanov, A. S.; Howard, J. A. K.; Hazendonk, P. *Eur. J. Org. Chem.* **2001**, 749−757.

Scheme 1 [a]

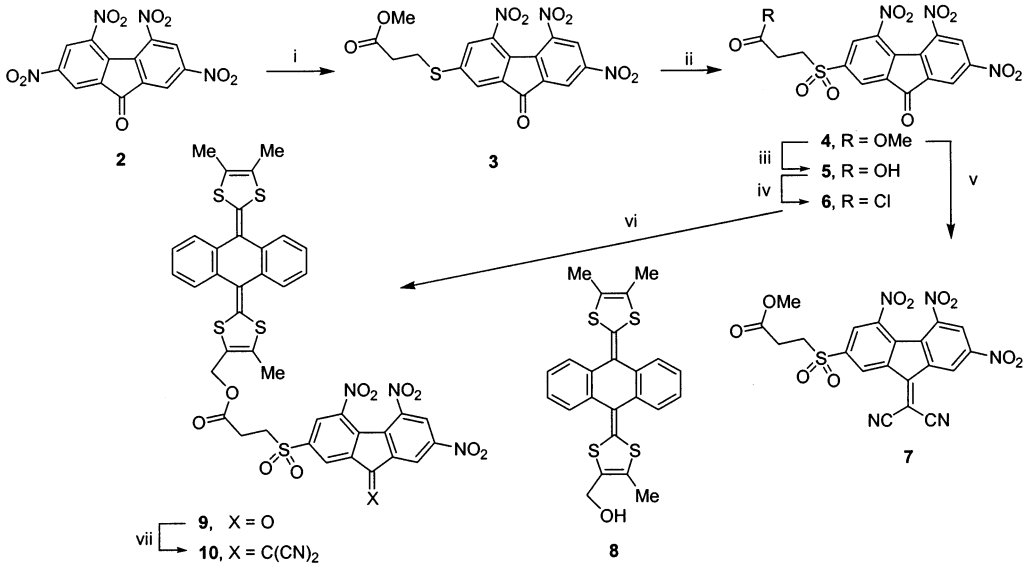

[a] Reagents and conditions: (i) $HSCH_2CH_2CO_2Me$ + $NaHCO_3$/MeCN, 20 °C, 6 h; (ii) H_2O_2/AcOH, 60 °C, 3.5 h; (iii) CF_3CO_2H/H_2O, reflux, 4 h; (iv) $(COCl)_2/CH_2Cl_2$, 20 °C, 40 h; (v) $CH_2(CN)_2$/ DMF, 20 °C, 10−20 h; (vi) **6** + **8**, pyridine/THF, 20 °C, 12 h; (vii) $CH_2(CN)_2$/DMF, 20 °C, 12 h.

Scheme 2 [a]

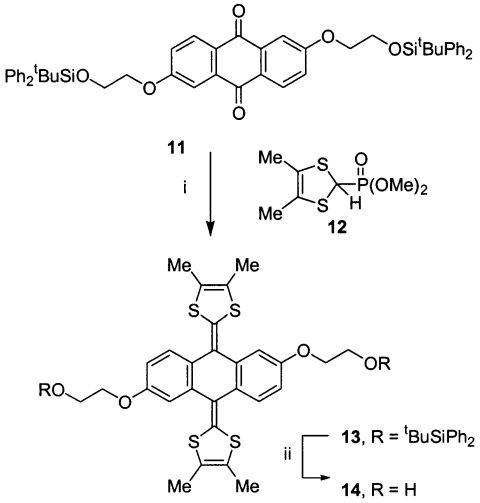

[a] Reagents and conditions: (i) **12** + LDA/THF, −78 °C, 1 h, then **11**, −78 °C → 20 °C, 12 h; (ii) Bu_4NF /THF, 20 °C, 1.5 h, then H_2O.

Scheme 3 [a]

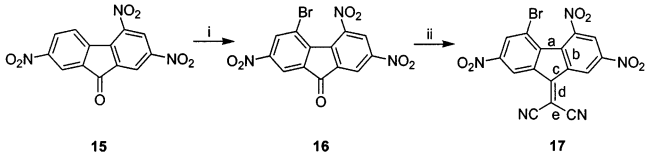

[a] Reagents and conditions: (i) $Br_2/H_2SO_4/HNO_3$, 55−60 °C, 2 h; (ii) $CH_2(CN)_2$/DMF, 20 °C, 2 h.

photeric multiredox behavior (Figure 1, Table 1), consisting of three reversible single-electron reduction waves (corresponding to the fluorene moiety)[24] and one two-electron quasireversible oxidation of the TTFAQ fragment. Therefore, five redox states have been observed, and are listed as follows: neutral (D^0/A^0), dication (D^{2+}/A^0), radical anion ($D^0/A^{\bullet-}$), dianion (D^0/A^{2-}), and radical trianion ($D^0/A^{\bullet 3-}$) for **9** and **10**; $A^0/D^0/A^0$, $A^0/D^{2+}/A^0$, $A^{\bullet-}/D^0/A^{\bullet-}$, $A^{2-}/D^0/A^{2-}$, $A^{\bullet 3-}/D^0/A^{\bullet 3-}$ states for **20** (for **19,** possessing the lower EA, the radical trianion state is not stable). The oxidation/reduction current ratio was 2:1 for compounds **9** and **10** and 1:1 for compounds **19** and **20,** as expected for their D/A stoichiometries.

The modification of fluorenone **9** to dicyanomethylene derivative **10** significantly increases its acceptor properties: The first reduction is shifted to a less negative value by ca. 0.3 V (Table 1), making the $E_{ox}^{pa} - E_{red}^{pa}$ gap as low as 0.25 V (anodic peak potentials were used instead of E_{red}^0 due to quasireversibility of the oxidation wave). When a solution of compound **10** was scanned negatively from +0.75 V (where the donor fragment exists in the dication state) the first reduction wave of the fluorene fragment merges with the reduction wave of the $TTFAQ^{2+}$ fragment, giving rise to a three-electron wave ($D^{2+}/A^0 + 3e \rightarrow D^0/A^{\bullet-}$) (Figure 1). This arises from the large separation between the anodic and cathodic oxidation peaks (≫59 mV) due to the quasireversibility of the TTFAQ oxidation. Moreover, the separation can be further increased at low temperature and/or at high scan rate.[15]

These observations led us to consider an intriguing idea: Could this reduction wave of the $TTFAQ^{2+}$ moiety be shifted to a more negative potential than the first reduction of the fluorene unit? If so, this could then result in the generation of a sixth, hitherto unknown, redox state: $D^{2+}/A^{\bullet-}$. Indeed, by varying the experimental conditions (scan rate and temperature) we have found that on the cathodic scan the $D^{2+} \rightarrow D^0$ wave can be distinctively seen to occur *after* the $A^0 \rightarrow A^{\bullet-}$ wave even at 0 °C and scan rates higher than 500 mV s^{-1}. A more clear example at −15 °C and scan rate 300 mV s^{-1} is shown in Figure 2. However, the low-temperature electrochemistry of **10** in MeCN (and also in CH_2Cl_2) is complicated by adsorption phenomena (e.g., the sharpness and intensity of the −0.7 V peak $D^{2+}/A^{\bullet-} \rightarrow D^0/A^{\bullet-}$ in Figure 2 are enhanced by adsorption).

To study in more detail the generation of the unusual species $D^{2+}/A^{\bullet-}$, we undertook an investigation of the electrochemistry of **10** in THF solution (where the adsorption processes are diminished) at different temperatures, concentrations, and scan

(23) For synthetic details see the Supporting Information. A similar oxidation reaction giving the TTF radical cation salt was also observed under these conditions for 4-hydroxymethyl-TTF (ref 37).
(24) Only two reversible reductions have been observed for **19**.

Scheme 4 [a]

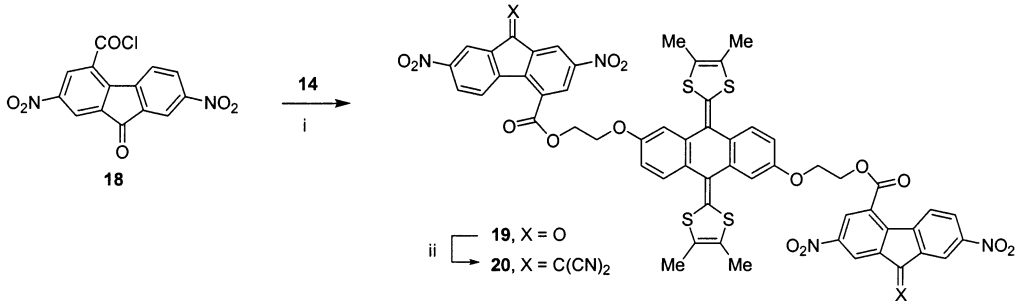

[a] Reagents and conditions: (i) pyridine/THF, 20 °C, 24 h; (ii) $CH_2(CN)_2$/DMF, 35 °C, 24 h.

Table 1. Redox Potentials in CH_2Cl_2 (ca. 10^{-4} M) vs Fc/Fc^+ (20 °C, 0.2 M nBu_4NPF_6)

compound	E_{ox}^{pa}/V	E_{ox}^{pc}/V	E_{1red}^{0}/V	E_{2red}^{0}/V	E_{3red}^{0}/V
4			−0.67	−1.04	−1.86
7			−0.31	−0.91	−1.57
8	−0.09	−0.32			
9	−0.07	−0.30	−0.65	−1.02	−1.85
10	−0.07	−0.33[a]	−0.35[a]	−0.94	−1.53
13	−0.13	−0.39			
14	−0.21	−0.32			
16			−0.77	−1.05	−1.85
17			−0.39	−0.93	−1.65
19	−0.11	−0.43	−1.05	−1.24	
20	−0.11	−0.43	−0.61	−1.15	−1.77

[a] These values could be determined only approximately due to an overlap of E_{ox}^{pc} and E_{1red}^{pc}.

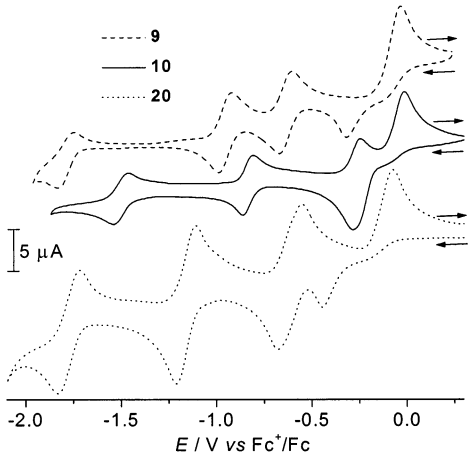

Figure 1. CV of compounds **9**, **10,** and **20** in MeCN, 0.1 M nBu_4NPF_6.

rates and performed a quantitative analysis of the experimental data. Controlled potential electrolysis (at the potential of the anodic peak) of model TTFAQ **8** in THF consumes two electrons per molecule and confirms a two-electron process. As above, the CV of **10** in THF exhibits three reversible one-electron reduction processes (only the first two were subjected to analysis). The electrochemical potentials of these reduction waves are independent of scan rate, concentration, and temperature. In the positive direction, there is only one oxidation peak and one reduction peak on the return sweep with a very large separation between them, which increases with lowering the temperature and with increasing the scan rate (Figure 3).

Thus, at +20 °C the reduction step of the $TTFAQ^{2+}$ moiety occurs at the potential of the first reduction step of the fluorene. Therefore, the single electron reduction at the first cycle ($D^0/A^0 \rightarrow D^0/A^{\bullet-}$) is turned into a three-electron reduction at this potential on the succeeding cycles ($D^{2+}/A^0 \rightarrow D^0/A^{\bullet-}$), as

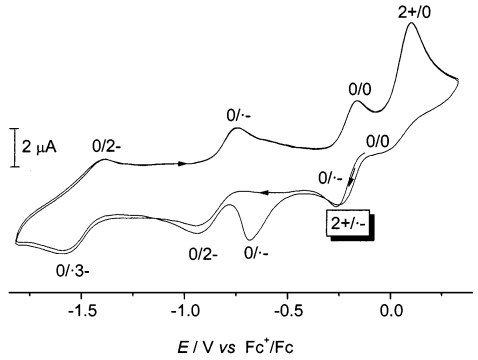

Figure 2. CV of compound **10** in MeCN at −15 °C, scan rate 300 mV s^{-1} (0.1 M nBu_4NPF_6) and a schematic representation of the electrochemical reactions. The notation on the redox peaks refers to the redox state of the donor/acceptor units, respectively, at that potential.

confirmed by the increase in current (Figure 3, left column). At −20 °C, however, the two-electron reduction of $TTFAQ^{2+}$ moiety ($D^{2+} \rightarrow D^0$) is shifted to a more negative region and occurs between the first ($A^0 \rightarrow A^{\bullet-}$) and the second reduction steps ($A^{\bullet-} \rightarrow A^{2-}$) of the fluorene moiety (Figure 3, right column). Therefore, the current values at E^{pc} for the first cycle ($D^0/A^0 \rightarrow D^0/A^{\bullet-}$) and the succeeding cycles of D^{2+}/A^0 reduction almost coincide, confirming single electron processes ($A^0 \rightarrow A^{\bullet-}$) in both cases. Consequently, a $D^{2+}/A^{\bullet-}$ species is generated on the return sweep (sweeping from D^{2+}/A^0).

Oxidation of **10** is a typical example of inverted potentials in a two-electron process;[25] i.e., it is easier to remove the second electron than the first. The reason for this is the tremendous gain in aromaticity in formation of the dication, which does not occur for the radical cation. The significant conformational change accompanying this transformation explains the relative slowness of this process, which is manifested in a large separation between the corresponding anodic and cathodic peaks. The oxidation process can be described by the following equations:

$$D^{\bullet+}-A + e^- \rightleftharpoons D-A \qquad (E_{ox1}, k_{ox1}, \alpha_{ox1})$$

$$D^{2+}-A + e^- \rightleftharpoons D^{\bullet+}-A \qquad (E_{ox2}, k_{ox2}, \alpha_{ox2}) \text{ and } E_{ox2} < E_{ox1}$$

$$2D^{\bullet+}-A \rightleftharpoons D^{2+}-A + D-A \qquad (K_{disp}, k_{disp}, k_{cop})$$

and the reduction steps are composed of three reversible single-electron transfers ($D-A/D-A^{\bullet-}$, $D-A^{\bullet-}/D-A^{2-}$, $D-A^{2-}/D-A^{\bullet 3-}$).

(25) Kai, H.; Evans, D. H. *J. Electroanal. Chem.* **1997**, *423*, 29−35.

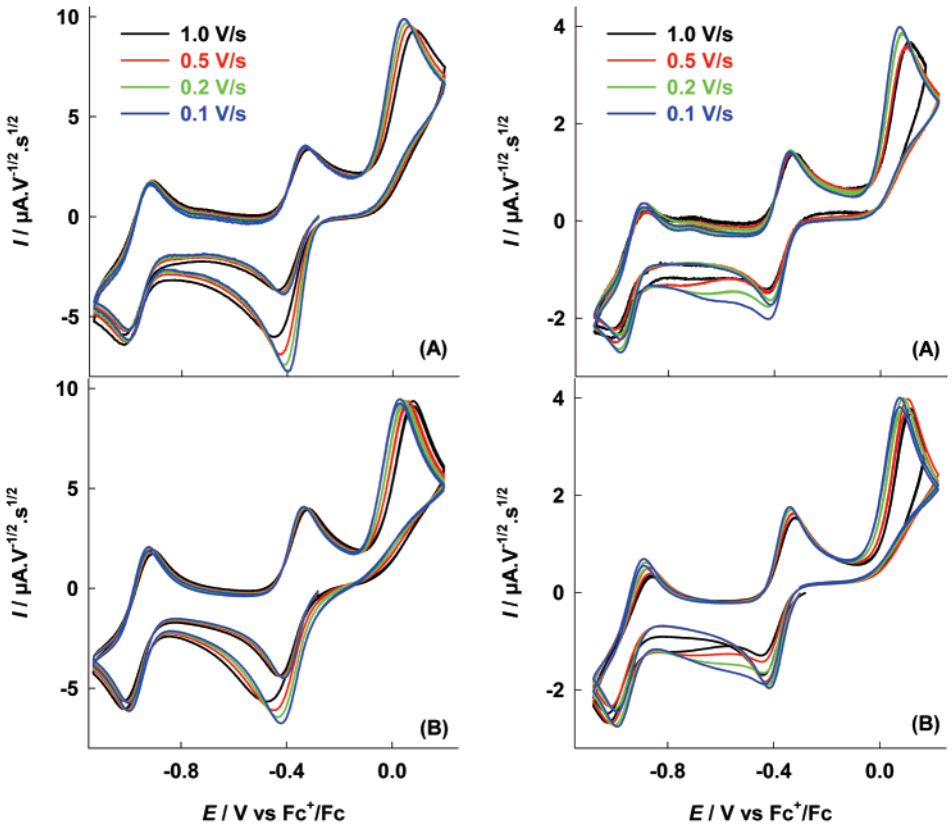

Figure 3. Experimental (A) and simulation (B) voltammograms for 0.6 mM **10** in 0.2 M nBu$_4$NPF$_6$/THF at +20 °C (left column) and at −20 °C (right column).

Table 2. Redox Potentials and Electron Transfer Parameters[a] for Compound **10** Estimated by Fitting with Digisim 3.05'

			redox process			
T/°C	D[b]/cm^2 s^{-1}		D–A$^{\bullet-}$/D–A^{2-}	D–A/D–A$^{\bullet-}$	D$^{\bullet+}$–A/D–A	D^{2+}–A/D$^{\bullet+}$–A
+20	3.8×10^{-6}	E°/V	−0.955	−0.375	0.01[c]	−0.09[c]
		α	0.5	0.5	0.55[d]	0.40[d]
		k/cm s^{-1}	1.0×10^{-2}	1.0×10^{-2}	1.0×10^{-2}	1.0×10^{-4}
0	3.1×10^{-6}	E°/V	−0.945	−0.375	0.03[c]	−0.12[c]
		α	0.5	0.5	0.60[d]	0.30[d]
		k/cm s^{-1}	0.8×10^{-2}	0.8×10^{-2}	0.8×10^{-2}	0.8×10^{-4}
−20	2.4×10^{-6}	E°/V	−0.945	−0.375	0.04[c]	−0.15[c]
		α	0.5	0.5	0.65[d]	0.25[d]
		k/cm s^{-1}	0.6×10^{-2}	0.6×10^{-2}	0.6×10^{-2}	0.60×10^{-4}
−45	1.8×10^{-6}	E°/V	−0.950	−0.375	0.07[c]	−0.20[c]
		α	0.5	0.5	0.70[d]	0.15[d]
		k/cm s^{-1}	0.1×10^{-2}	0.1×10^{-2}	0.1×10^{-2}	0.1×10^{-4}

[a] Potentials E° vs Fc/Fc$^+$ (0.5 mM substrate in 0.1 M nBu$_4$NPF$_6$/THF); α is an electron-transfer coefficient; k is an electron-transfer rate constant. [b] Diffusion coefficient; it was set the same for all the redox states. [c] These values were imposed according to the procedure of ref 25. [d] These values are standard in inverted potentials in a two-electron process: ref 25.

A quantitative analysis of the data over the scan rate range and the temperature range investigated was carried out with Digisim 3.05. Good simulation fits were found for scan rates from 0.1 to 5.0 V s^{-1} at +20, 0, −20, and −45 °C (Table 2 and Figure 3).[26] Agreement was improved at faster scan rates by inclusion of the disproportionation reaction with $k_{disp} = 10^6$ M^{-1} s^{-1}, although this does not provide an accurate assessment of this parameter (Table 2).

Thus, the CV experiments demonstrate clear evidence for existence of the $D^{2+}/A^{\bullet-}$ state for compound **10**, and parameters found from simulation confirm faster kinetics for reduction of the fluorene moiety in the D^{2+}/A^0 state vs the TTFAQ moiety.

We note that the difference in electrochemical kinetics between two sites in one molecule having close redox potentials was recently used in the design of a bifunctional molecule that receives two electrons sequentially through only one of its two electroactive groups.[27] Also, it was recently shown that in carotenoids (which play an important role in photosynthesis[28]) an inversion of the standard potentials for the first and second electron transfer substantially depends on the structure.[29] Therefore, our finding of redirection of electron transfer to the thermodynamically less favorable site by changing electro-

(26) CVs for the scan rates from 0.1 to 1.0 V only are shown on Figure 3 for clarity.

(27) Zheng, Z.-R.; Evans, D. H. *J. Am. Chem. Soc.* **1999**, *121*, 2941−2942.
(28) (a) Frank, H. A.; Cogdell, R. J. In *Carotenoids in Photosynthesis*; Young, A., Britton, G., Eds.; Chapman and Hall: London, 1993; Chapter 8, p 252. (b) Faller, P.; Pascal, A.; Rutherford, A. W. *Biochemistry* **2001**, *40*, 6431−6440.

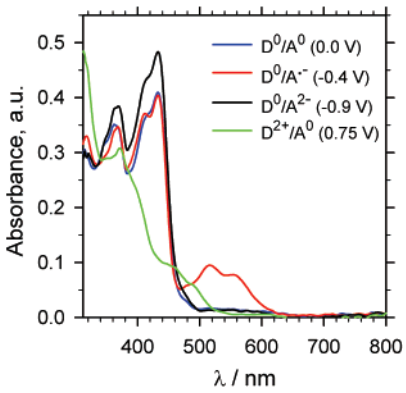

Figure 4. UV−vis spectroelectrochemistry for compound **10** in thin layer conditions ($d \approx 100$ μm, +20 °C).

chemical kinetic factors may be important for studying electron transfer in biosystems.[29,30]

Spectroelectrochemistry. To support our conclusions on the unusual electrochemistry of **10** we performed UV−vis spectral characterization of $D^0/A^{\bullet-}$, D/A^{2-}, and D^{2+}/A^0 redox states. Figure 4 demonstrates reflection−absorption spectra for compound **10** in the neutral state (D^0/A^0) as well as $D^0/A^{\bullet-}$, D/A^{2-}, and D^{2+}/A^0 redox states at room temperature. The neutral state is featured by two peaks at 362 and 432 nm (the last shows also a shoulder at ca. 415 nm), characteristic for the TTFAQ nucleus.[16d] These remain essentially unchanged on reduction to $D^0/A^{\bullet-}$ ($\lambda_{max} = 368$, 412, and 432 nm with near the same intensity), and the wavelengths are essentially unchanged with higher intensity on further reduction to D/A^{2-} ($\lambda_{max} = 369$, 412 (sh), and 432 nm). Additional absorptions at 515 and 550 (sh) nm from the radical anion of the fluorene moiety emerge for $D^0/A^{\bullet-}$, but then disappear for the D/A^{2-} state. A similar absorption spectrum ($\lambda_{max} = 470$, 515, and 550 nm) was recently observed for the electrochemically generated radical anion of TTF-σ-fluorene diad **1**.[11b] On oxidation to D^{2+}/A^0, the peak at 368 nm decreases, and the peak at 432 nm almost completely disappears, whereas low intense broad absorption is observed as shoulders at 460 and 490 nm.

Because the $D^{2+}/A^{\bullet-}$ species was observed in CV only as a transient at low temperatures, we performed comparative simultaneous CV−UV−vis spectral (time-resolved SEC) experiments for **10** at +20 °C and at −30 °C, in thin-layer conditions at scan rate 5−10 mV/s[31] (in reflection spectral mode). Figure 5 shows evolution of the spectrum during the cyclic voltammetry at +20 °C: starting from the neutral state D^0/A^0 and sweeping the potential to the negative direction, the first cycle results in reversible formation of $D^0/A^{\bullet-} \rightarrow D^0/A^{2-}$ → (reverse sweep direction) → $D^0/A^{\bullet-} \rightarrow D^0/A^0 \rightarrow D^{2+}/A^0$ species with their characteristic absorptions. A spectrum of the neutral D^0/A^0 state was used as a background (yellow color at zero point time), so negative absorption at 360−470 nm for D^{2+}/A^0 is due to consumption of D^0/A^0 (Figure 4). The second cycle (300−600 s on time scale) essentially repeats the evolution of the spectrum, confirming the reversibility of all redox processes.

The same time-resolved SEC experiment at −30 °C indicates that on the first cycle, the evolution of the spectrum is the same as at +20 °C, i.e., reversible formation $D^0/A^{\bullet-} \rightarrow D^0/A^{2-} \rightarrow D^0/A^{\bullet-} \rightarrow D^0/A^0 \rightarrow D^{2+}/A^0$ species (Figure 6). However, it becomes clearly different on the second cycle, starting from the D^{2+}/A^0 species. At +20 °C, the second cycle showed sharp transition from D^{2+}/A^0 (disappears at $E = -0.25$ V ($t = 325$ s), Figure 5A,B) to $D^0/A^{\bullet-}$ (appears at $E = -0.35$ V ($t = 335$ s)) with possible existence of D^0/A^0 in the narrow potential region. At −30 °C, however, a specific potential window displays both a negative absorption in the short-wavelength region (360−470 nm) characteristic for the D^{2+} moiety and a low-intensity, but visible, positive absorption at 480−570 nm, characteristic for the $A^{\bullet-}$ moiety. Thus at 700 s, which corresponds to $E_{pc} = -0.3$ V for the reduction of the D^{2+}/A^0 species (Figure 6A), the negative absorption at 360−470 nm corresponding to D^{2+} moiety has not yet disappeared (Figure 6B) and remains observable until ca. $E = -0.75$ V ($t = 790$ s), whereas a longer wavelength absorption at 500−550 nm starts to appear at $E = -0.50$ V ($t = 740$ s). We attribute this to the existence of the transient species $D^{2+}/A^{\bullet-}$, which is expected to combine the spectral characteristics of the D^{2+} and $A^{\bullet-}$ moieties. As the CV profile (Figure 6A) shows no good resolution between $D^{2+}/A^0 \rightarrow D^{2+}/A^{\bullet-}$ and $D^{2+}/A^0 \rightarrow D^0/A^0$ processes, the coexistence of $D^{2+}/A^{\bullet-}$, D^0/A^0, and $D^0/A^{\bullet-}$ species is possible. Also, due to the method limitation for these time-resolved SEC experiments [thin-layer (TL) conditions, low scan rate, low substrate concentration to avoid an adsorption] the concentration of $D^{2+}/A^{\bullet-}$ species in the solution was much lower than that in the CV experiment preventing its precise spectral characterization. Nevertheless, the characteristic short-wavelength negative absorption at 730−790 s does support our conclusions on the generation of $D^{2+}/A^{\bullet-}$ in the CV experiment.

As follows from the CV of **10** at low temperature (Figure 3), the two-electron reduction $D^{2+} \rightarrow D^0$ occurs as a very broad peak overlapping with the single-electron reduction $A^0 \rightarrow A^{\bullet-}$ and extending into the next reduction step ($A^{\bullet-} \rightarrow A^{2-}$). In the time-resolved SEC experiments at −30 °C, this results in decreased absorption (at 400−500 nm) from the D^0/A^{2-} species at $E \approx -0.8$ to −0.9 V ($t = 800$−840 s) (positive absorption from A^{2-} is compensated by negative absorption from D^{2+}), whereas an oxidation on the back scan ($D^0/A^{2-} \rightarrow D^0/A^{\bullet-} \rightarrow D^0/A^0 \rightarrow D^{2+}/A^0$) nicely reproduces the spectral features of all consequent redox states (Figure 6B).

IR Spectra. The solid-state IR spectral studies (in KBr pellets) show that the C≡N stretching frequency of compound **10**, $\nu_{C\equiv N} = 2185$ cm^{-1} (and a second very weak signal at 2154 cm^{-1}), is at significantly lower wavenumber as compared to that in a neutral fluorene moiety (represented by compounds **7** and **21**, $\nu_{C\equiv N} = 2233$ cm^{-1}) and is consistent with that of the ion radical salt (**21**$^{\bullet-}$)Li$^+$ (2185 cm^{-1}).[11b] A similar change in the C≡N stretching frequency from 2225 to 2180 cm^{-1} was also found for the $TCNQ^0/TCNQ^{\bullet-}$ system.[32,33] The CN

(29) An inversion of the standard potentials for the first and second electron transfer substantially depends on the structure of carotenoids: an inversion occurs in the oxidation of β-carotene and in the reduction of canthaxanthin, but not in the reduction of β-carotene or in the oxidation of canthaxanthin: Hapiot, P.; Kispert, L. D.; Konovalov, V. V.; Savéant, J.-M. *J. Am. Chem. Soc.* **2001**, *123*, 6669−6677.

(30) Dwyer, T. M.; Mortl, S.; Kemter, K.; Bacher, A. Fauq, A.; Frerman, F. E. *Biochemistry* **1999**, *38*, 9735−9745.

(31) A higher scan rate which would provide a higher concentration of $D^{2+}/A^{\bullet-}$ species could not be achieved in the thin layer SEC cell due to an increase in the uncompensated resistance, especially in a low-polar solvent (e.g., THF, which was used to prevent the adsorption of the D^{2+}/A^0 species) and at low electrolyte concentration (to prevent its precipitation at low temperatures).

(32) Chappell, J. S.; Bloch, A. N.; Bryden, W. A.; Maxfield, M.; Poehler, T. O.; Cowan, D. O. *J. Am. Chem. Soc.* **1981**, *103*, 2442−2447.

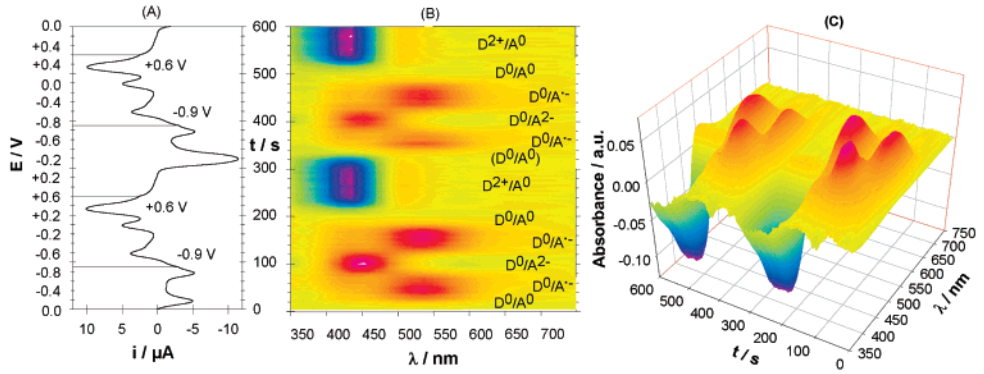

Figure 5. Time-resolved UV−vis spectroelectrochemistry for compound **10** in thin layer conditions ($d \approx 50$ μm, +20 °C), in 2D (B) and 3D (C) presentation. CV conditions (A): scan rate 10 mV/s, potentials range −0.9 to +0.6 V, vs Ag wire scanning in the negative direction starting at 0 V.

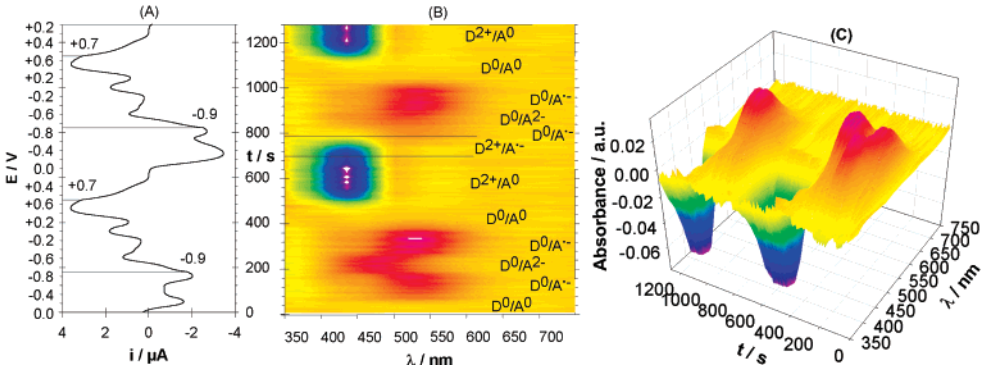

Figure 6. Time-resolved UV−vis spectroelectrochemistry for compound **10** in thin layer conditions ($d \approx 50$ μm, −30 °C), in 2D (B) and 3D (C) presentation. CV conditions (A): scan rate 5 mV/s, potentials range −0.9 to +0.7 V, vs Ag wire scanning in the negative direction starting at 0 V.

Chart 2

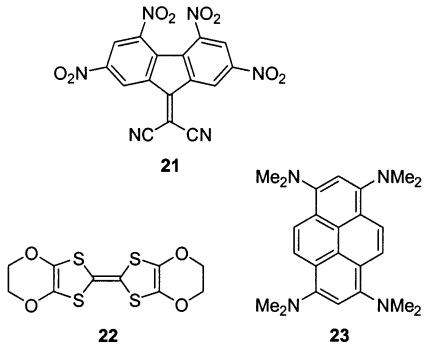

stretching frequencies for **10** are in excellent agreement with $\nu_{C\equiv N}$ = 2185 and 2154 cm^{-1} found for the ionic conductive complex of a similar fluorene with BEDO−TTF (**22**)$_2$·**21**.[34] Similar values of the C≡N stretching were obtained for another ionic complex, (**21**)$_2$·**23** (2182 cm^{-1}),[33] whereas an increase of $\nu_{C\equiv N}$ to 2203 cm^{-1} was observed in TTF−fluorene CTC with partial charge transfer, **21**·TTF[11b] (for neutral acceptor **21** $\nu_{C\equiv N}$ = 2233 cm^{-1}). These data suggest a complete electron transfer in the diad **10** with formation of the fluorene radical anion in the solid state. This conclusion is in full agreement with X-ray analysis (see below) of the CTC **14**·(**17**)$_2$ (the C≡N frequencies of which are almost identical to those of **10**) where the TTFAQ and fluorene components exist as the dication and radical anion species, respectively. The further lowering of the C≡N stretching frequency for the weaker band at 2154 cm^{-1} in **10** and **14**·(**17**)$_2$ may indicate more negative charge accumulated on the cyano groups, as would be the case for a dianion species. Due to the lower electron affinity of the acceptor moiety in compound **20** there is a small shift of the C≡N peak (to $\nu_{C\equiv N}$ = 2227 cm^{-1}) due to much weaker charge transfer in this compound.

A key difference between **10** and **14**·(**17**)$_2$, apart from the covalent linkage of the donor and acceptor components in the former, is the different D/A stoichiometry. The 1:2 D/A ratio in complex **14**·(**17**)$_2$ satisfies the two-electron donor and one-electron acceptor characteristics of the components, whereas this is not the case for **10**, where the D/A ratio was designed to be 1:1. This dilemma is solved in the solid state by intermolecular interaction with another fluorene moiety from an adjacent molecule accepting the second electron from the TTFAQ moiety. However, in solution the donor and acceptor fragments of one molecule are expected to interact intramolecularly only, which should result in very different CT behavior. Unfortunately, the extremely low intensity of the CN signal in solution (an IR spectrum of **10** in CH_2Cl_2 shows no significant absorption in the region expected for the CN group, Figure S2 in Supporting Information)[35] prevented a detailed investigation of this interesting point.

(33) Saito, G.; Hirate, S.; Nishimura, K.; Yamochi, H. *J. Mater. Chem.* **2001**, *11*, 723−735.
(34) Horiuchi, S.; Yamochi, H.; Saito, G.; Sakaguchi, K.; Kusunoki, M. *J. Am. Chem. Soc.* **1996**, *118*, 8604−8622.
(35) We also observed a dramatic decrease in the intensity of the CN stretching in the IR spectra in solution (compared to that in KBr pellets) for other fluorene-9-dicyanomethylene acceptors, e.g., for compounds **7** ν_{CN} = 2233 cm^{-1} as an extremely weak band. Variation of the solvent did not restore the peak intensity. A marked variation in the intensity of CN absorption from strong to undetectable in different solvents and with the incorporation of certain substituents is well documented: Bellamy, L. J. In *The infrared spectra of complex molecules*, 3rd ed.; Chapman and Hall: London and New York, 1975; Vol. 1, p 297.

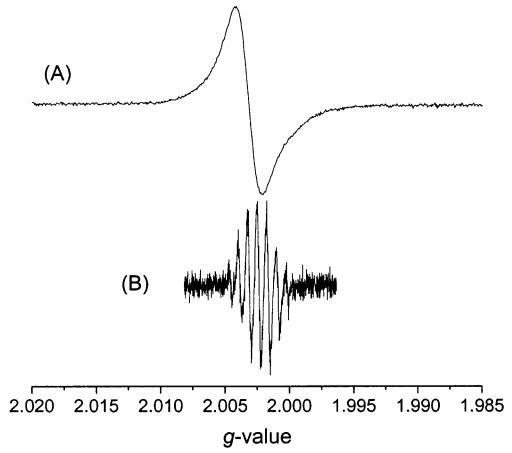

Figure 7. EPR spectrum of **10** in CH_2Cl_2 at 105 K (A) and in 0.1 M Bu_4NPF_6/THF at 298 K (B).

Electron Paramagnetic Resonance (EPR) Studies. The high donor and acceptor ability of the TTFAQ and fluorene moieties, respectively, in **10** results in the appearance of new properties in this donor−acceptor diad. Whereas isolated TTFAQ **8** and fluorene **7** are both EPR silent (as expected), facile electron transfer in **10** results in a strong EPR signal in the solid state and a less intense signal in solution. It also manifests in paramagnetic broadening of the signals in the ^{1}H NMR spectra for protons adjacent to the fluorene nucleus of **10** (but not for **9**, **19,** and **20** which possess weaker acceptor moieties). Since the TTFAQ radical cation is not stable[16d] (it rapidly disproportionates to form the diamagnetic dication $TTFAQ^{2+}$), only one EPR signal is expected, corresponding to the radical anion of the fluorene moiety. Indeed, both acetone and CH_2Cl_2 solutions as well as a powdered sample (even at Q-band frequency) give a broad single line[36] centered at $g = 2.0028-2.0034$ which is close to the measured g-value of the ion radical salt (**21**$^{\bullet-}$)Li^+ [37] (TTF-like radical cations have $g \approx 2.007$ in fluid solution[38]). When a CH_2Cl_2 solution is cooled to 250 K, a poorly resolved hyperfine structure is observed, but the signal broadens on further cooling, and on freezing to 105 K, a single line is observed at $g = 2.0034$ (Figure 7A). Spin-counting experiments reveal that only ca. 1% of the molecules exist in a radical form in CH_2Cl_2 solution at room temperature, thus indicating an essentially neutral ground state for **10** in solution.[39] Despite the low radical concentration, we believe that the EPR signal in solution is a result of electron transfer in compound **10** itself and not due to impurity. Most probably, electron transfer occurs only in the donor−acceptor complexed state (head-to-tail intramolecular or intermolecular, or a combination of those CTCs), which is stable in the solid state but easily dissociates in solution.

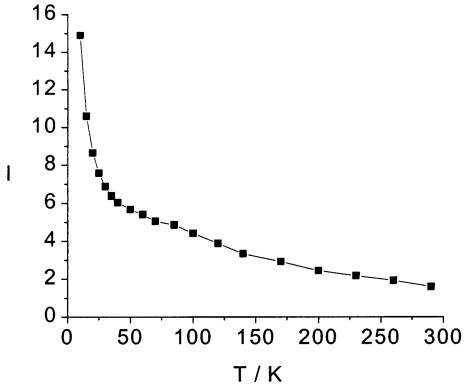

Figure 8. Temperature dependence of the intensity of the EPR signal of **10** in the solid state.

EPR experiments for **10** in 0.2 M nBu_4NPF_6/THF solution showed hyperfine structure of the spectrum even at room temperature ($g = 2.0024$), although the signal was very weak (Figure 7B). The spectrum observed is very similar to that of the ion radical salt (**21**$^{\bullet-}$)Li^+,[37] which displays hyperfine coupling to two sets of two equivalent ^{14}N nuclei ($a_{2N} = 3.25$ and 0.51 MHz, respectively) and two sets of two equivalent ^{1}H nuclei ($a_{2H} = 3.38$ and 0.14 MHz, respectively, from EPR and electron nuclear double resonance measurements). We assigned the larger of the two ^{1}H couplings to the 3 and 6 positions of the fluorene ring. The EPR spectrum of **10** can be simulated with two equivalent ^{14}N (3.4 MHz) and two equivalent ^{1}H nuclei (3.4 MHz).[40] By analogy with (**21**$^{\bullet-}$)Li^+, we assign the ^{1}H coupling to the 3,6 positions of the fluorene. Even though these are no longer chemically equivalent in **10**, an SO_2R group has a very similar electronic influence to NO_2,[41] and we do not resolve the difference between the two sites.

Simultaneous electrochemistry and EPR (SEEPR) experiments for the above solution were performed by continuous scanning of the potential from +0.8 to −0.2 V vs Ag wire at 1000 mV/s to generate a quasistationery concentration of D^0/$A^{\bullet-}$ and D^{2+}/$A^{\bullet-}$ radicals in the EPR cell (see Supporting Information).[42] The population of the D^{2+}/$A^{\bullet-}$ species was expected to increase with lowering the temperature. However, there was no significant difference in the spectral shape or position for +20, −10, and −40 °C and only a small increase in intensity was observed (as expected for ground-state radicals). We attribute this signal to the D^0/$A^{\bullet-}$ radical anion. Thus, we were unable to register the transient D^{2+}/$A^{\bullet-}$ species by SEEPR spectroscopy, which could be due to the fact that its signal is very similar to that of D^0/$A^{\bullet-}$.

Variable-temperature studies on powdered samples of **10** show that the intensity of the signal increases monotonically with decreasing temperature down to 10 K (Figure 8), indicating a ground (not thermoexcited) state character of the radical species. The ionic CTC **14**$^{\bullet}$(**17**)$_2$ gives rise to almost the same EPR spectra: A single line corresponding to the fluorene radical anion was found in the solid state ($g = 2.0031$) and a similar,

(36) A much less (1/10) intense signal at $g = 2.007$ (the value expected for a TTF-like radical cation) was also observed at 300 K in CH_2Cl_2 only. Given its very low concentration and the fact that it disappears on changing the solvent, concentration, or temperature, we cannot unambiguously assign this signal.

(37) Perepichka, D. F.; Bryce, M. R.; Batsanov, A. S.; McInnes, E. J. L.; Zhao, J. P.; Farley, R. D. *Chem. Eur. J.* **2002**, *8*, 4656−4669.

(38) (a) Ribera, E.; Rovira, C.; Veciana, J.; Tarrés, J.; Canadell, E.; Rousseau, R.; Molins, E.; Mas, M.; Schoeffel, J.-P.; Pouget, J.-P.; Morgado, J.; Henriques, R. T.; Almeida, M. *Chem. Eur. J.* **1999**, *5*, 2025−2039. (b) Cavara, L.; Gerson, F.; Cowan, D. O.; Lerstrup, K. *Helv. Chim. Acta* **1986**, *69*, 141−151.

(39) The free radical concentration in the solid state was estimated at 298 K by spin counting experiment to be ca. 15%, as a result of antiferromagnetic interaction between neighboring fluorene moieties. Lowering of the observed spin number (in respect to the theoretical value) is typical for many radical ion salts, e.g., ref 3b.

(40) The significantly larger line width of **10,** cf. (**21**$^{\bullet-}$)Li^+, precludes observation of the smaller couplings.

(41) Hansch, C.; Leo, A.; Taft, R. W. *Chem. Rev.* **1991**, *91*, 165−195.

(42) Fast scanning of the potential with continuous recording of the spectra was employed as a practically achievable alternative to time-resolved pulse SEEPR.

though less intense, signal in CH_2Cl_2[36] ($g = 2.0029$) and acetone ($g = 2.0027$) solutions. Taking into account the results of X-ray studies (see below) and IR spectroscopy, it is evident that a full electron transfer giving rise to the fluorene radical anion and dication of TTFAQ in the solid state of the diad **10** and the CTC **14**·(**17**)$_2$. Due to the 1:1 donor/acceptor ratio in **10**, the TTFAQ moiety in this diad presumably exists as a mixture of the neutral and dication states, which is also consistent with the UV−vis spectrum of **10** in solid films (see below). The stability of this charge-separated species can be explained by aromatic stabilization of the $TTFAQ^{2+}$ [43] unit and also by increased crystalline forces for the ionic molecules.

Another manifestation of the CT character of these compounds is their pronounced electrical conductivity. Both compound **10** and complex **14**·(**17**)$_2$ show very similar conductivity values: $\sigma_{rt} = 2 \times 10^{-6}$ and 8×10^{-6} S cm^{-1}, respectively (two-probe method on compressed pellets). This conductivity of **10** is quite high for a single-component purely organic monomeric material,[3,12,44] although substantially higher values (10^{-2} S cm^{-1}) have been reported recently.[45]

CT Complexation in Solution and in the Solid State. Examination of the electronic absorption spectra of compounds **9** and **10** in different solvents (CH_2Cl_2, $CHCl_3$, MeCN) revealed only very weak CT interaction for both compounds. There were very broad weak bands (Figure S3 in Supporting Information) in the region ca. 500−1300 nm ($\lambda_{max} \approx 650$ nm, $\epsilon \approx 60$ M^{-1} cm^{-1}) for **9** and ca. 500−2000 nm (λ_{max} 780 and 1150 nm, $\epsilon \approx 50$ M^{-1} cm^{-1}, in CH_2Cl_2) for **10**. A linear dependence was found in the concentration range 5×10^{-4} to 5×10^{-3} M consistent with the intramolecular character of these bands.[46] Taking into account the EPR data, it is very likely that absorption of the fluorene radical anion contributes to the long-wavelength bands of **10**.[47] This behavior is in contrast to the analogous TTF−σ−fluorene diad **1**,[11b] where the ICT band ($\lambda_{max} = 1230$ nm) is considerably more intense ($\epsilon = 4700$ M^{-1} cm^{-1}). The reason for this difference is probably a highly bent geometry of the TTFAQ moiety, which prevents efficient π-complexation between the donor and acceptor fragments in **10**. In the solid state, however, the UV−vis spectrum of **10** (see Supporting Information) shows very strong long-wavelength absorbance consistent with superposition of $TTFAQ^0$, $TTFAQ^{2+}$,[16d] and fluorene$^{\bullet-}$ [11b] characteristic bands (see also SEC part) but with no peak at 1150 nm for a CT band (as observed in solution).

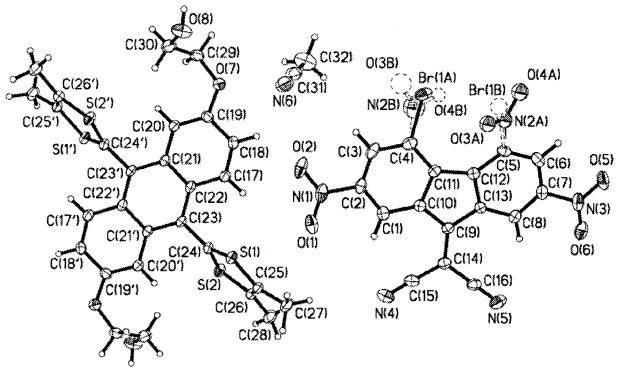

Figure 9. Dication, radical anion, and solvent in the crystal structure of **14**·(**17**)$_2$·2MeCN.

This is in agreement with suggested disproportionation of **10** in the solid state to give a mixture of D^{2+}−σ−$A^{\bullet-}$ and D^0−σ−$A^{\bullet-}$.

A solution of the intermolecular CT complex **14**·(**17**)$_2$ in THF (1.5×10^{-3} M) does not give any observable long-wavelength absorption band due to dissociation of the complex. However, a strong donor−acceptor interaction in the solid state of this complex results in full electron transfer with formation of dication **14**$^{2+}$ and two radical anions **17**$^{\bullet-}$ as confirmed by X-ray analysis. It presents the first definite example of a fully ionic fluorene CTC.[48] This is in contrast to analogous CTCs TTF·**17** and Me_3BrTTF·**17** which show only partial charge transfer (see Supporting Information). In the structure of **14**·(**17**)$_2$·2MeCN, the $TTFAQ^{2+}$ unit has crystallographic C_i symmetry, while the fluorene and the acetonitrile molecule of crystallization occupy general positions (Figure 9). As with other TTFAQ systems,[16] the conformation of **14** drastically changes on oxidation: The folded anthracenediylidene moiety is converted into a planar (within ±0.03 Å), fully aromatic anthracene system (details of the X-ray structural analysis of isolated **14** and **17** are given in Supporting Information). Each dithiole ring acquires a +1 charge, which is manifested in the shortening of C−S bonds (ca. 1.68−1.72 Å) and lengthening of the C=C bonds (1.360(4) Å) in the dithiole ring (for more details see Table S1 in Supporting Information), as well as planarization of the ring (Figure 9). The correlation between positive charge and C−S distances is well studied for TTF,[49] and the same approach can be applied to TTFAQ (e.g., in 2,6-dibutoxy-9,10-bis(1,3-dithiol-2-ylidene)-9,10-dihydroanthracene, C(2)−S(1), C(3)−S(1), and C(3)=C(4) distances are of 1.770(3), 1.745(3), and 1.319(4) Å, respectively, for the neutral state and of 1.680(2), 1.710(2), and 1.346(3) Å, respectively, in its charge-transfer salt with $TCNQ_2$·2MeCN).[16c] Thus, the dithiole ring in **14**$^{2+}$ has essentially the same geometry as that in $(TTFMe_4)(ClO_4)_2$.[50] The

(43) Although formation of cation radical also yields one aromatic dithiolium ring, the largest gain of aromaticity occurs on transition from cation radical (which essentially preserves the geometry of the neutral species) to fully aromatic dication: (a) Reference 16d. (b) Martín, N.; Sánchez, L.; Seoane, C.; Ortí, E.; Viruela, P. M.; Viruela, R. *J. Org. Chem.* **1998**, *63*, 1268−1279.

(44) (a) Inokuchi, H.; Imaeda, K.; Enoki, T.; Mori, T.; Marayama, Y.; Saito, G.; Okada, N.; Seki, K.; Higuchi, Y.; Yasuoka, N. *Nature* **1987**, *329*, 39−40. (b) Cordes, A. W.; Haddon, R. C.; Oakley, R. T.; Schneemeyer, L. F.; Waszczak, J. V.; Young, K. M.; Zimmerman, N. M. *J. Am. Chem. Soc.* **1991**, *113*, 582−588. (c) Yamashita, Y.; Tanaka, S.; Imaeda, K.; Inokuchi, H. *Chem. Lett.* **1991**, 1213−1216. (d) Cordes, A. W.; Haddon, R. C.; Oakley, R. T. *Adv. Mater.* **1994**, *6*, 798−802.

(45) (a) Chi, X.; Itkis, M. E.; Patrick, B. O.; Barclay, T. M.; Reed, R. W.; Oakley, R. T.; Cordes, A. W.; Haddon, R. C. *J. Am. Chem. Soc.* **1999**, *121*, 10395−10402. (b) Chi, X.; Itkis, M. E.; Kirschbaum, K.; Pinkerton, A. A.; Oakley, R. T.; Cordes, A. W.; Haddon, R. C. *J. Am. Chem. Soc.* **2001**, *123*, 4041−4048.

(46) The low accuracy accompanying measurements of such weak bands does not exclude the possibility that intermolecular complexation may contribute to these absorption bands.

(47) The radical anion of the fluorene moiety has moderately intense bands in the region 500−2000 nm ($\epsilon_{800\ nm} \approx 4 \times 10^{-3}$ M^{-1} cm^{-1}, ref 11b and 37), and $TTFAQ^{2+}$ does not absorb beyond 600 nm (ref 16d).

(48) All the known X-ray crystal structures of nitrofluorene−TTFs CTCs are neutral or have only partial charge transfer: (a) Reference 21. (b) Perepichka, I. F.; Perepichka, D. F.; Lyubchik, S. B.; Bryce, M. R.; Batsanov, A. S.; Howard, J. A. K. *J. Chem. Soc., Perkin Trans. 2* **2001**, 1546−1551. (c) Bryce, M. R.; Moore, A. J.; Batsanov, A. S.; Howard, J. A. K.; Robertson, N. R.; Perepichka, I. F. In *Supramolecular Engineering of Synthetic Metallic Materials: Conductors and Magnets*; Veciana, J., Rovira, C., Amabilino, D. B., Eds.; NATO ASI Series; Kluwer Publishers: Dordrecht, 1999; Vol. 518, pp 437−449. (d) Perepichka, I. F.; Kuz'mina, L. G.; Perepichka, D. F.; Bryce, M. R.; Goldenberg, L. M.; Popov, A. F.; Howard, J. A. K. *J. Org. Chem.* **1998**, *63*, 6484−6493. (e) Moore, A. J.; Bryce, M. R.; Batsanov, A. S.; Heaton, J. N.; Lehmann, C. W.; Howard, J. A. K.; Robertson, N.; Underhill, A. E.; Perepichka, I. F. *J. Mater. Chem.* **1998**, *8*, 1541−1550. (f) Soriano-García, M.; Toscano, R. A.; Robles Martínez, J. G.; Salmerón, U. A.; Lezama R. R. *Acta Crystallogr.* **1989**, *C45*, 1442−1444.

(49) Clemente, D. A.; Marzotto, A. *J. Mater. Chem.* **1996**, *6*, 941−946.

dithiolium and anthracene systems form a dihedral angle of 62° and are connected by the essentially single C(23)−C(24) bond of 1.488(4) Å (1.34(2) Å for the neutral state, see Table S1 in Supporting Information).[51] Comparison of the **17**$^{\bullet-}$ anion with the neutral molecule (Table S1 in Supporting Information) shows a shortening of the previously single bonds a, c, and e (Scheme 3) and lengthening of the b and c bonds, resulting in a nearly uniform delocalization of π-electron density in the five-membered fluorene ring and the dicyanomethylene group. These changes resemble those which occur on reduction of TCNQ to the anion radical.[52] The Br and NO_2 substituents are disordered between positions 4 and 5, in an 85(A):15(B) ratio (similar "4/5 disorder" occurs in every structure studied, reducing the precision). Repulsion between these substituents causes the fluorene system to warp, but slightly less than that in neutral **17**. The average deviation of the 13 carbon atoms from their mean plane is 0.08 Å, with a maximum deviation of 0.19 Å. There is a 7° twist around d.

Conclusions

We have shown that extended-TTF donors and fluorene acceptors can be used as convenient synthons in the design of D−σ−A systems with high amphotericity. We have synthesized TTFAQ−σ−fluorene diad **10** and have demonstrated that it displays clear multistage redox behavior (three single-electron reduction and one two-electron oxidation processes): $E_{ox} - E_{red}$ is as low as 0.25 V, which is to the best of our knowledge the lowest known value for closed shell D−σ−A systems. It has been demonstrated by CV experiments on diad **10**, and supported by time-resolved UV−vis spectroelectrochemistry, that under certain conditions a previously unknown D^{2+}−σ−$A^{\bullet-}$ redox state can been generated. This finding represents an important example of preferable kinetically controlled electron transfer onto a thermodynamically less favorable center, which suggests a new approach for controlling electron-transfer processes. In contrast to TTF−fluorene intermolecular CTCs and D−σ−A diads, the donor−acceptor interaction between the TTFAQ and the fluorene moieties in the solid state results in complete one-electron transfer, as demonstrated by X-ray analysis (for the intermolecular complex **14**·(**17**)$_2$), Fourier transform infrared spectroscopy (FTIR), and EPR data [for **10** and **14**·(**17**)$_2$]. In solution, however, only a low-spin concentration (1%) and no CT absorption were observed for **10,** indicating the facile dissociation of the complex.

Experimental Section

General details are the same as described previously.[53] UV−vis−near-IR spectra were recorded on Varian Cary 5 spectrophotometer.

Electrochemistry. Cyclic voltammetric experiments have been carried out at 298 and 253 K (±0.1 K) with EG&G PAR 273A potentiostat/galvanostat or BAS CV50 electrochemical analyzers in a three-electrode cell (Ag/Ag^+ reference). The working electrodes were 1, 1.6, or 2 mm diameter platinum disks polished to a mirror finish. Platinum wire was used as an auxiliary electrode. An ohmic drop compensation was applied when necessary. Numerical simulations of the voltammograms were performed with Digisim 3.05 using the default numerical options with the assumption of planar diffusion. The Butler−Volmer law was applied for the electron-transfer kinetics.

Spectroelectrochemistry. Routine UV−vis SEC experiments have been performed with a Perkin-Elmer Lambda 19 NIR spectrometer. Time-resolved spectroelectrochemistry was performed using the reported experimental setup.[54] In both cases, CV was performed in thin-layer conditions (50−100 μm) using 0.1 M nBu$_4$NPF$_6$/THF as an electrolyte, and spectra were recorded in reflection mode using a Pt disk 5 mm in diameter as working electrode and a reflector and Ag wire as a quasireference electrode. For each experiment, the samples (cell and solution) were prepared in a glovebox containing dry, oxygen-free (<1 ppm) argon.

EPR Experiments. X- and Q-band EPR spectra were recorded on a Bruker EMX and a Bruker ESP 300E spectrometer, respectively. The solid-state variable-temperature (300−10 K) studies on **10** were performed at Q-band under nonsaturating conditions determined at 10 K (0.1 mW microwave power; 100 kHz and 5 G modulation frequency and amplitude, respectively). Spin-counting experiments on **10** in degassed CH_2Cl_2 were performed at X-band and room temperature by calibration against a range of concentrations of standard 2,2-di(4-*tert*-octylphenyl)-1-picrylhydrazyl solutions in benzene measured under identical, nonsaturating conditions. The experimental protocol was tested for accuracy against solutions of known concentration of other radical species.

SEEPR experiments were carried out on a Bruker ESP 300 spectrometer driven by Bruker's ESP 1600 software. The design of the SEEPR-electrochemical cell was inspired by the work of Fiedler et al.[55] Experiments were performed in the X-band frequency range (~9.4 GHz) in a TE102 cavity. Low-temperature measurements involved a standard variable-temperature cryostat using liquid nitrogen evaporation. The samples (cell and solution) were prepared in a glovebox containing dry, oxygen-free (<1 ppm) argon.

Methyl 3-(4,5,7-Trinitro-9-oxo-2-fluorenylsulfanyl)propanoate (3). To a solution of fluorenone **2** (2.00 g, 5.62 mmol) in acetonitrile (200 mL), finely powdered $NaHCO_3$ (2.0 g, 24 mmol) was added, followed by methyl 3-mercaptopropionate (1.5 mL, 14 mmol). The reaction mixture was stirred at 20 °C for 6 h, then left at 0 °C for 15 h. The complete consumption of the starting fluorenone was confirmed by thin-layer chromatography. The reaction mixture was filtered from the inorganic salts, concentrated in vacuo to ca. 15 mL, and diluted with hot propan-2-ol (50 mL). The yellow precipitate which formed on cooling was filtered off, washed with propan-2-ol and with water, and dried in vacuo, giving pure sulfide **3** (1.86 g, 76%), mp 163−165 °C.[56] *m*/*z* (EI): 433 (M^+, 11%), 149 (100%). ^{1}H NMR (200 MHz, $CDCl_3$): δ 8.93 (1H, d, J = 2 Hz), 8.75 (1H, d, J = 2 Hz), 7.95 (1H, d, J = 2 Hz), 7.92 (1H, d, J = 2 Hz), 3.75 (3H, s), 3.42 (2H, t, J = 7 Hz), 2.79 (2H, t, J = 7 Hz). ^{13}C NMR (75 MHz, $CDCl_3$): δ 185.8, 171.1, 151.1, 148.6, 147.1, 146.9, 145.5, 139.5, 137.61, 137.56, 128.5, 127.0, 125.51, 125.50, 122.4, 52.3, 33.0, 27.4. Anal. Calcd for $C_{17}H_{11}N_3O_9S$: C, 47.12; H, 2.56; N, 9.70. Found: C, 46.76; H, 2.54; N, 9.73.

Methyl 3-(4,5,7-Trinitro-9-oxo-2-fluorenylsulfonyl)propanoate (4). To a hot solution of sulfide **3** (0.43 g, 0.92 mmol) in acetic acid (15 mL), H_2O_2 (33% aqueous solution; 0.7 mL) was added and the reaction mixture was stirred at 60 °C for 3.5 h. The solution was then concentrated in vacuo to 5−7 mL, and the hot solution was diluted

(50) Shibaeva, R. P. *Kristallografiya* **1984**, *29*, 480−484 (in Russian).
(51) Similar changes in C(2-dithiole)−C(9-anthracene) distances for the neutral and the charged states were observed for other TTFAQ derivatives: donor **21** (1.366(3) Å) and its charge-transfer salt **21**·TCNQ$_2$·2MeCN (1.486(2) Å), (ref 16c); 2,6-di(2-hydroxyethoxy)-9,10-bis[4,5-di(methylthio)-1,3-dithiol-2-ylidene]-9,10-dihydroanthracene **(22)** (1.361(4) Å) and **22**$^{2+}$·(ClO_4^-)$_2$ (1.487(6) Å) (ref 16e).
(52) (a) Flandrois, S.; Chasseau, D. *Acta Crystallogr*. **1977**, *B33*, 2744−2750. (b) Kistenmacher, T. J.; Emge, T. J.; Bloch, A. N.; Cowan, D. O. *Acta Crystallogr*. **1982**, *B38*, 1193−1199.
(53) Moore, A. J.; Chesney, A.; Bryce, M. R.; Batsanov, A. S.; Kelly, J. F.; Howard, J. A. K.; Perepichka, I. F.; Perepichka, D. F.; Meshulam, G.; Berkovich, G.; Kotler, Z.; Mazor, R.; Khodorkovsky, V. *Eur. J. Org. Chem.* **2001**, 1927−1935.
(54) Gaillard, F.; Levillain, E. *J. Electroanal. Chem.* **1995**, *398*, 77−87.
(55) Fiedler, D. A.; Koppenol, M.; Bond, A. M. *J. Electrochem. Soc.* **1995**, *142*, 862−867.
(56) An additional portion of **3** (100 mg, 4%) can be isolated from the mother liquor by flash chromatography on silica, eluting with CH_2Cl_2, mp 158−160 °C.

with water (3 mL) and cooled in an ice bath. The precipitate was filtered off, washed sequentially with water and $NaHCO_3$ solution, then with hot water, and, finally, with methanol (1 mL), giving sulfone **4** (0.42 g, 90%), mp 187−188 °C. *m/z* (EI): 465 (M^+, 5%), 379 (100%). *m/z* (CI): 483 ($[MNH_4]^+$, 85%), 453 (100%). ^{1}H NMR (200 MHz, acetone-d_6): δ 9.05 (1H, d, J = 2 Hz), 8.86 (1H, d, J = 2 Hz), 8.76 (1H, d, J = 2 Hz), 8.64 (1H, d, J = 2 Hz), 3.87 (2H, t, J = 7.5 Hz), 3.62 (3H, s), 2.86 (2H, t, J = 7.5 Hz). ^{13}C NMR (75 MHz, acetone-d_6): δ 185.4, 170.9, 151, 147.4, 147.2, 144.8, 139.8, 139.7, 138.3, 137.8, 131.5, 128.4, 126.7, 123.4, 52.4, 51.6, 28.1. IR (KBr): ν 1741 (C═O), 1620 (C═O), 1544, 1367, 1348, 1317 cm^{-1}. Anal. Calcd for $C_{17}H_{11}N_3O_{11}S$: C, 43.88; H, 2.38; N, 9.03. Found: C, 43.62; H, 2.32; N, 8.98.

3-(4,5,7-Trinitro-9-oxo-2-fluorenylsulfonyl)propanoic Acid (5). Ester **4** (0.40 g, 0.86 mmol) was dissolved in a mixture of trifluoroacetic acid (4 mL) and water (4 mL) and refluxed for 4 h (a white precipitate formed after 0.5−1 h). After the mixture cooled, the precipitate was filtered off and washed with hot water and methanol affording acid **5** as a white powder (0.39 g, 100%), mp 247 °C (dec). *m/z* (EI): 451 (M^+, 24%), 379 ($[M-CH_2CH_2CO_2]^+$, 100%). ^{1}H NMR (200 MHz, acetone-d_6): δ 9.05 (1H, d, J = 2 Hz), 8.86 (1H, d, J = 2 Hz), 8.76 (1H, d, J = 2 Hz), 8.65 (1H, d, J = 2 Hz), 3.85 (2H, t, J = 7.5 Hz), 2.85 (2H, t, J = 7.5 Hz). Anal. Calcd for $C_{16}H_9N_3O_{11}S$: C, 42.58; H, 2.01; N, 9.31. Found: C, 42.40; H, 1.96; N, 9.32.

3-(4,5,7-Trinitro-9-oxo-2-fluorenylsulfonyl)propanoyl Chloride (6). To a suspension of acid **5** (100 mg, 0.22 mol) in dry CH_2Cl_2 (2 mL), oxalyl chloride (1 mL, excess) and *N*,*N*-dimethylformamide (DMF) (2 μL) were added and the reaction mixture was stirred for 40 h. The solvent was removed in vacuo, and the residue was suspended in dry CH_2Cl_2 (1 mL), filtered off, washed with CH_2Cl_2 (2 mL), and dried in a flow of Ar, giving acid chloride **5b** (105 mg, 100%), which was used in the next step without purification. ^{1}H NMR (300 MHz, acetone-d_6): δ 9.05 (1H, d, J = 2 Hz), 8.86 (1H, d, J = 2 Hz), 8.80 (1H, d, J = 2 Hz), 8.68 (1H, d, J = 2 Hz), 4.03 (2H, t, J = 7.5 Hz), 3.63 (2H, t, J = 7.5 Hz).

Methyl 3-(9-Dicyanomethylene-4,5,7-trinitro-2-fluorenylsulfonyl)-propanoate (7). A solution of fluorenone **4** (61 mg, 0.13 mmol) and malononitrile (31 mg, 0.47 mmol) in DMF (0.5 mL) was stirred at 20 °C for 6 h and then left at 0 °C overnight. The dark green reaction mixture was diluted with MeOH (3 mL) and stirred at 0 °C for 1 h, and the precipitate was filtered off and washed with MeOH. The yellow-greenish powder was dissolved in hot acetone (1.5 mL), diluted with MeOH (3 mL), and left to crystallize at 0 °C, giving pure product **7** (50 mg, 75%), mp 240 °C (dec). *m/z* (EI): 513 (M^+, 4%), 389 (100%). MS (CI): *m/z* 531 (MNH_4^+, 16%), 274 (100%). ^{1}H NMR (300 MHz, acetone-d_6): δ 9.74 (1H, d, J = 2 Hz), 9.44 (1H, d, J = 2 Hz), 9.10 (1H, d, J = 2 Hz), 8.82 (1H, d, J = 2 Hz), 3.86 (2H, t, J = 7.5 Hz), 3.62 (3H, s), 2.89 (2H, t, J = 7.5 Hz). ^{13}C NMR (75 MHz; acetone-d_6): δ170.8, 154.1, 150.3, 147.7, 147.4, 144.2, 140.0, 139.7, 135.3, 134.6, 130.8, 130.0, 126.0, 125.0, 113.2, 113.1, 85.9, 52.24, 51.9, 28.1. IR (KBr): ν 2233 (C≡N), 1736 (C═O), 1545, 1344 cm^{-1}. Anal. Calcd for $C_{20}H_{11}N_5O_{10}S$: C, 46.79; H, 2.16; N, 13.64. Found: C, 46.76; H, 2.13; N, 13.67.

Fluorenone 9. To a solution of acid chloride **6** (118 mg, 0.250 mmol) in dry THF (6 mL) at −20 °C, pyridine (23 μL, 0.285 mmol) and then a solution of alcohol **8**[22] (106 mg, 0.225 mmol) in THF (10 mL) were added and the reaction mixture was stirred at −20 °C for 2 h and then stirred overnight at 20 °C. The solvent was then removed in vacuo, and the residue was chromatographed on silica, eluting with CH_2Cl_2. The main gray-yellow fraction was evaporated, and the residue was stirred with petroleum ether and filtered giving a brown solid of **9** (160 mg, 80%), mp 210 °C (dec). *m/z* (FAB): 885 (M^+, 55%), 123 (100%). ^{1}H NMR (300 MHz, $CDCl_3$): δ 9.00 (1H, d, J = 2 Hz), 8.83 (1H, d, J = 2 Hz), 8.67 (1H, d, J = 2 Hz), 8.58 (1H, d, J = 2 Hz), 7.59−7.67 (2H, m), 7.49−7.57 (2H, m), 7.20−7.32 (4H, m), 4.82 (1H, d, J = 13 Hz), 4.70 (1H, d, J = 13 Hz), 3.58 (2H, t, J = 7 Hz), 2.90 (2H, t, J = 7 Hz), 2.00 (3H, s), 1.927 (3H, s), 1.921 (3H, s). IR (KBr): ν 1739 (C═O), 1617 (C═O), 1541, 1443, 1343 cm^{-1}. Anal. Calcd for $C_{40}H_{27}N_3O_{11}S_5$: C, 54.23; H, 3.07; N, 4.74. Found: C, 54.11; H, 3.23; N, 4.61.

Dicyanomethylenefluorene 10. To a solution of fluorenone **9** (52 mg, 0.059 mmol) in dry DMF (0.5 mL), malononitrile (30 mg, 0.45 mmol) was added and the mixture was stirred at 20 °C for 12 h, after which period it was diluted with methanol and left for 2−3 h at 0 °C. The precipitate was then filtered, washed with methanol, and dried in vacuo. The resulting brown powder was extracted with dry $CHCl_3$ (4 × 5 mL), the extract was evaporated, and the residue was taken up in CH_2Cl_2. This solution was stirred for 1−2 min with dry silica (10 mg)[57] and filtered. The silica was then washed with CH_2Cl_2,[58] and the filtrate was evaporated and dried in vacuo, giving pure product **10** (47 mg, 86%), mp > 300 °C. *m/z* (ES): 933 (M^+, 100%). ^{1}H NMR (300 MHz, $CDCl_3$): δ 9.74 (1H, s), 9.39 (1H, s), 9.04 (1H, br), 8.70 (1H, br), 7.59−7.67 (2H, m), 7.48−7.57 (2H, m), 7.20−7.32 (4H, m), 4.82 (1H, d, J = 13 Hz), 4.70 (1H, d, J = 13 Hz), 3.62 (2H, t, J = 7 Hz), 2.94 (2H, t, J = 7 Hz), 2.00 (3H, s), 1.92 (6H, s). IR (KBr): ν 2185 (C≡N), 2154 (C≡N), 1741 (C═O), 1541, 1445, 1342 cm^{-1}. Anal. Calcd for $C_{43}H_{27}N_5O_{10}S_5$: C, 55.30; H, 2.91; N, 7.50. Found: 55.10; H, 2.98; N, 7.54.

2,6-Bis{2-[(*tert*-butyldiphenylsilyl)oxy]ethoxy}-9,10-bis(4,5-dimethyl-1,3-dithiol-2-ylidene)-9,10-dihydroanthracene (13). To a solution of the phosphonate ester **12**[59] (4.15 g, 17.3 mmol) in dry THF (200 mL) at −78 °C under argon was added lithium diisopropylamide (1.5 M solution in cyclohexane; 12.7 mL, 19.0 mmol), and the resultant cloudy yellow-brown mixture was stirred for 1 h at −78 °C. Anthraquinone **11**[16e] (5.56 g, 6.90 mmol) was dissolved in dry THF (50 mL) and added to the reaction mixture via a syringe over 30 min. The reaction mixture was stirred at −78 °C for another 1 h, whereupon it was allowed to attain room temperature over 12 h. Evaporation of the solvent gave a red residue which was dissolved in CH_2Cl_2 (300 mL), washed with water and brine, dried ($MgSO_4$), and concentrated in vacuo. Column chromatography (silica gel, CH_2Cl_2−hexane, 1:1 v/v) afforded **13** as a yellow foam (4.13 g, 58%), mp 128−131 °C (from $CHCl_3$−methanol). *m/z* (EI): 1032 (M^+, 100%). ^{1}H NMR ($CDCl_3$): δ 7.76−7.74 (8H, m), 7.52 (2H, d, J = 8.5 Hz), 7.43−7.38 (12H, m), 7.18 (2H, d, J = 2.5 Hz), 6.77 (2H, dd, J_1 = 2.5 Hz, J_2 = 8.5 Hz), 4.17 (4H, t, J = 5 Hz), 4.04 (4H, t, J = 5 Hz), 1.92 (6H, s), 1.91 (6H, s), 1.09 (18H, s). ^{13}C NMR ($CDCl_3$): δ 156.7, 136.8, 135.6, 133.6, 131.2, 129.6, 128.3, 127.7, 126.3, 121.2, 120.8, 120.6, 111.7, 111.2, 69.2, 62.6, 26.8, 19.2, 13.10, 13.07. Anal. Calcd for $C_{60}H_{64}O_4S_4Si_2$: C, 69.72; H, 6.24. Found: C, 69.46; H, 6.24.

2,6-Bis(2-hydroxyethoxy)-9,10-bis(4,5-dimethyl-1,3-dithiol-2-ylidene)-9,10-dihydroanthracene (14). Compound **13** (3.70 g, 3.57 mmol) was dissolved in dry THF (50 mL), and a solution of tetrabutylammonium fluoride (10.7 mL, 10.7 mmol of a 1.0 M solution in THF) was added dropwise over 15 min, causing the reaction mixture to change color from yellow to brown. Further stirring for 1.5 h, followed by addition of water (0.1 mL) and evaporation of the solvent, afforded a brown residue. It was dissolved in CH_2Cl_2 (200 mL), washed with water and brine, dried ($MgSO_4$), and concentrated in vacuo. Chromatography using a short column (silica gel, initially CH_2Cl_2 to remove the byproducts, then CH_2Cl_2−acetone, 9:1 v/v) afforded **14** as a yellow powder (1.65 g, 83%), mp 218−220 °C (dec). *m/z* (EI): 556 (M^+, 100%). ^{1}H NMR ($CDCl_3$): δ 7.53 (2H, d, J = 8.5 Hz), 7.17 (2H, d, J = 2.5 Hz), 6.81 (2H, dd, J 8.5 and 2.5 Hz), 4.15 (4H, t, J = 4.5 Hz), 4.01−3.98 (4H, m), 2.06 (2H, t, J = 6.0 Hz), 1.923 (6H, s), 1.916 (6H, s). ^{13}C NMR ($CDCl_3$): δ 156.4, 136.9, 131.7, 128.7, 126.5 (2C),

(57) Hydrolysis of compound **10** to fluorenone **9** on silica (which we have not observed for other fluorene-9-dicyanomethylene derivatives) does not allow chromatographic purification.
(58) Sometimes compound **10** (and also **9**) is retained on silica; in this case, a few drops of methanol were added to CH_2Cl_2 to elute all the compound.
(59) Moore, A. J.; Bryce, M. R. *J. Chem. Soc., Perkin Trans. 1* **1991**, 157−168.

120.9, 120.8, 111.5, 111.4, 69.3, 61.5, 13.2, 13.1. Anal. Calcd for $C_{28}H_{28}O_4S_4$: C, 60.40; H, 5.07. Found: C, 60.15; H, 5.06.

4-Bromo-2,5,7-trinitrofluorene-9-one (16).[60] Fluorenone **15** (5.00 g, 15.9 mmol) was dissolved in a mixture of fuming nitric acid (5.3 mL, 127 mmol; $d = 1.51$ g mL^{-1}) and concentrated sulfuric acid (150 mL; $d = 1.84$ g mL^{-1}) with heating at 50 °C. Bromine (13.0 g, 81 mmol) was added dropwise over 10 min, and the mixture was stirred at 55−60 °C for 2 h. The mixture was cooled to ambient temperature and poured onto 1 kg of crushed ice. The solid was filtered off and washed with water yielding compound **16** (5.70 g, 91%). Recrystallization of this crude product by dissolution in acetic acid (65 mL) and further addition of hot water (15 mL) afforded pure **16** (3.65 g, 58%), mp 194−195 °C (191−192 °C).[61] ^{1}H NMR (300 MHz, acetone-d_6): δ 8.97 (1H, d, $J = 2$ Hz), 8.80 (1H, d, $J = 2$ Hz), 8.76 (1H, d, $J = 2$ Hz), 8.55 (1H, d, $J = 2$ Hz). ^{13}C (50 MHz, acetone-d_6): δ 185.8 (C═O), 150.9, 150.4, 145.6, 140.5, 140.2, 139.9, 136.3, 126.4, 122.4, 121.7, 118.9.

4-Bromo-2,5,7-trinitro-9-dicyanomethylenefluorene (17). Fluorenone **16** (500 mg, 1.27 mmol) and malononitrile (180 mg, 2.73 mmol) in DMF (2.0 mL) were stirred at ambient temperature for 2 h (immediate dissolution followed by precipitation in 30 min). The mixture was diluted with ethanol (8 mL) and allowed to stay at +5 °C for 3 h. The solid was filtered off and washed with ethanol affording compound **17** (530 mg, 94%), mp 340 °C (dec) (MeCN). *m*/*z* (CI$^-$): 442, 440 ([M − H]$^-$, 100%, 100%). ^{1}H NMR (200 MHz, acetone-d_6 + 0.5 drop of CF_3CO_2D): δ 9.66 (1H, d, $J = 2$ Hz), 9.47 (1H, d, $J = 2$ Hz), 9.03 (1H, d, $J = 2$ Hz), 8.86 (1H, d, $J = 2$ Hz). ^{13}C (50 MHz, acetone-d_6): δ 158.8, 158.0, 154.9, 150.4, 142.7, 140.5, 140.0, 135.5, 125.9, 124.2, 122.1, 120.7, 118.7, 113.4, 113.3, 113.0. Anal. Calcd for $C_{16}H_4BrN_5O_6$: C, 43.46; H, 0.91; Br, 18.07; N, 15.84. Found: C, 43.34; H, 0.84; Br, 17.80; N, 15.77.

CTC 14·(17)$_2$. To the solution of acceptor **17** (18.0 mg, 41 mmol) in hot acetonitrile (1.2 mL), a solution of donor **14** (11.4 mg, 20 mmol) in acetonitrile (0.8 mL) was added, and the solution was left to stand. The black crystalline product was collected, washed with acetonitrile, and dried, affording CTC **14·(17)$_2$**. It was not possible to remove all the MeCN even by drying in vacuo at 100 °C. Anal. Calcd for $C_{60}H_{36}Br_2N_{10}O_{16}S_4 \cdot {}^1/_3$MeCN: C, 50.09; H, 2.56; N, 9.95. Found: C, 49.60; H, 2.53; N, 10.39. IR (KBr) ν: 2230 (MeCN), 2179 and 2153 (CN), 1625, 1580, 1511, 1445 1333, 1310, 1077 cm^{-1}.

Fluorenone 19. Carbonyl chloride **19** (157 mg, 0.45 mmol) and diol **14** (84 mg, 0.15 mmol) in dry THF (20 mL) were stirred under nitrogen until full dissolution. Dry pyridine (0.080 mL, 1.0 mmol) was added, and the solution was stirred at 20 °C for 24 h. It was diluted with H_2O and then extracted with CH_2Cl_2, the organic layer was washed with H_2O and dried, and the solvent was evaporated. Column chromatography (silica gel, CH_2Cl_2) of the residue (140 mg) afforded **19** (104 mg, 60%), mp >200 °C (dec). *m*/*z* (FAB): 1148 (M$^+$, 10%), 152 (100%). ^{1}H NMR (300 MHz, $CDCl_3$): δ 8.91 (2H, d, $J = 2.5$ Hz), 8.66 (2H, d, $J = 8.5$ Hz), 8.59 (2H, d, $J = 2.5$ Hz), 8.49 (2H, d, $J = 2$ Hz), 8.39 (2H, dd, $J = 8.5$ Hz, $J = 2.1$ Hz), 7.33 (2H, d, $J = 8.5$ Hz), 7.06 (2H, d, $J = 2.5$ Hz), 6.78 (2H, dd, $J = 8.5$ Hz, $J = 2.4$ Hz), 4.90 (4H, m), 4.49 (4H, m), 1.835 (6H, s), 1.827 (6H, s). ^{13}C NMR (75 MHz, $CDCl_3$): δ 187.6 (C═O), 164.2 (C═O), 156.0, 149.4, 148.5, 146.6, 146.0, 137.5, 136.8, 136.1, 132.5, 131.7, 130.3, 128.8, 128.7 (2C), 126.3, 122.0, 121.0, 120.7, 120.0, 119.2, 111.7, and 111.6 (dithiole C-4 and C-5), 65.9 and 65.3 (CH_2CH_2), 13.04 (CH_3), 13.00 (CH_3). IR (KBr) ν: 1732 (C═O), 1609, 1590, 1528 (NO_2), 1343 (NO_2), 1275, 1219, 1158, 1086, 737 cm^{-1}. Anal. Calcd for $C_{56}H_{36}N_4O_{16}S_4$: C, 58.53; H, 3.16; N, 4.88. Found: C, 58.46; H, 3.22; N, 4.97.

Dicyanomethylenefluorene 20. Fluorenone **19** (50 mg, 0.044 mmol) and malononitrile (10.5 mg, 0.159 mmol) in DMF (0.40 mL) were stirred at 35 °C for 24 h, the solvent was removed in high vacuum, and the residue was chromatographed (silica gel, CH_2Cl_2) affording dicyanomethylene derivative **20** (37 mg, 68%), mp 190−195 °C. *m*/*z* (FAB): 1244 (M$^+$, 50%), 613 (100%). ^{1}H NMR (300 MHz, $CDCl_3$): δ 9.47 (2H, d, $J = 2$ Hz), 9.29 (2H, d, $J = 2$ Hz), 8.88 (2H, d, $J = 2$ Hz), 8.52 (2H, d, $J = 8.5$ Hz), 8.35 (2H, dd, $J = 8.5$ Hz, $J = 2$ Hz), 7.27 (2H, d, $J = 8.5$ Hz), 7.05 (2H, d, $J = 2.5$ Hz), 6.81 (2H, dd, $J = 8.5$ Hz, $J = 2.5$ Hz), 4.95 (4H, m), 4.53 (4H, m), 1.880 (6H, s), 1.872 (6H, s). IR (KBr) ν (cm^{-1}): 2227 (C≡N), 1731 (C═O), 1602, 1529 (NO_2), 1342 (NO_2), 1272, 1164, 1102, 732.

Acknowledgment. We thank Dr. Francois X. Sauvage (CNRS UMR 8516, Lille) for his help with SEEPR experiments and the following for funding: EPSRC (D.F.P. and C.A.C.); The Royal Society for funding visits to Durham (I.F.P. and S.B.L.); The Royal Society of Chemistry for a Grant for International Authors (I.F.P.); The University of Durham (N.G.).

Supporting Information Available: Experimental details of the reaction of 2,5,7-trinitrofluorene-9-one-4-carbonyl chloride with TTFAQ **14**,^{1}H NMR spectrum for compound **20**, FTIR transmission spectra of compound **10** in KBr pellets and in CH_2Cl_2 solution, UV−vis−near-IR spectra of compounds **9** and **10**, EPR and SEEPR spectra of **10** in 0.1 M *n*Bu$_4$NPF$_6$/THF, the description of the X-ray structures of **14**·$^1/_2$PhMe, **17**·PhMe, **17**·TTF, and **17**·TTFMe$_3$Br (PDF) with a table of selected bond distances, experimental details of the X-ray analysis, X-ray crystallographic files in CIF format for compounds **14**·$^1/_2$PhMe, **17**·PhMe, **17**·TTF, **17**·TTFMe$_3$Br, and **14** (**17**)$_2$·2MeCN are available free of charge via the Internet at http://pubs.acs.org.

JA012518O

(60) Procedure adapted from: Andrievskii, A. M.; Gorelik, M. V.; Avidon, S. V.; Al'tman, E. Sh. *Russ. J. Org. Chem.* **1993**, *29*, 1519−1524; *Zh. Org. Khim*. **1993**, *29*, 1828−1834 (in Russian).

(61) Newman, M. S.; Blum, J. *J. Am. Chem. Soc.* **1964**, *86*, 5600−5602.